Accepted Manuscript

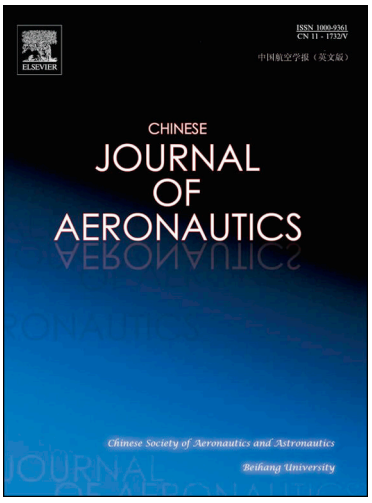

Full Length Article

Identification of crystal orientation for turbine blades with anisotropy materials

Yuanqiu Tan, Chaoping Zang, Biao Zhou, Xiaowei Wang, E.P. Petrov

PII: S1000-9361(17)30266-2
DOI: https://doi.org/10.1016/j.cja.2017.12.001
Reference: CJA 949

To appear in: *Chinese Journal of Aeronautics*

Received Date: 7 September 2016
Revised Date: 13 June 2017
Accepted Date: 16 October 2017

Please cite this article as: Y. Tan, C. Zang, B. Zhou, X. Wang, E.P. Petrov, Identification of crystal orientation for turbine blades with anisotropy materials, *Chinese Journal of Aeronautics* (2017), doi: https://doi.org/10.1016/j.cja.2017.12.001

Identification of crystal orientation for turbine blades with anisotropy materials

Yuanqiu TAN[a], Chaoping ZANG[a,*], Biao ZHOU [a], Xiaowei WANG[a], E.P. Petrov[b]

[a]*Jiangsu Province Key Laboratory of Aerospace Power System, Nanjing University of Aeronautics and Astronautics, Nanjing 210016, China*
[b]*University of Sussex, Brighton BN19QT, United Kingdom*

Received 7 September 2016; revised 13 June 2017; accepted 16 October 2017

Abstract

A novel approach to identify the crystal orientation of turbine blades with anisotropy materials is proposed. Based on enhanced mode basis, with the main advantages of its efficiency, accuracy and general applicability, the blade vibration mode of each order is linearly constructed by several specified mode shapes, which are obtained from the considered turbine blade with specified crystal orientations correspondingly. Then, a surrogate model based on Kriging method is introduced for constructing the condensed perturbed matrix of stiffness in order to improve the efficiency even further. The constructed surrogate model allows to perform the modal analysis of turbine blades with arbitrary crystal orientations in higher efficiency, due to the fact that the elements of condensed perturbed matrix of stiffness are considered in construction of the surrogate model rather than concerning the perturbation of all the elements of the initial stiffness matrix for the blade. Genetic algorithm is finally employed to optimize the defined fitness functions in order to identify the crystal orientation angles of turbine blades. Several corresponding examples demonstrated the accuracy, efficiency and general applicability of the proposed method.

Keywords: turbine blade; anisotropy materials; crystal orientation; surrogate model; genetic algorithm; identification

1. Introduction[1]

Turbine blades are operated on complex thermal and mechanical loads with thermal resistance, thermomechanical fatigue, creep and stress rupture problems[1-3]. In order to improve the performance capabilities of turbine blades in the operating environments such as high temperature and the conditions of high and low cycle fatigues, nickel-based superalloys are widely used as materials for gas turbine blades. Generally, nickel-based crystal superalloys include Single Crystal (SC) and Directionally Solidified (DS) alloys, and furthermore their materials are Face-Centred Cubic (FCC)[4]. The single crystal blade consists of one columnar grain and can be modelled as orthotropic material in the lattice directions, while the directionally solidified blade consists of several columnar grains and can be modelled as transverse isotropic by assuming that the number of the columnar grains included in the blade is large[5]. Nickel-based turbine blades are directionally solidified during the casting process with the crystallographic direction [0,0,1] aligned with the blade stacking axis *Z*. Practically, this alignment of blade stacking axis, *Z*, with crystal primary axis, [0,0,1], is variable and controlled within 15^{o}, known as the primary angle, marked as θ.[6]

*Corresponding author. *E-mail address:* c.zang@nuaa.edu.cn

Actually, the characteristics of dynamics, fatigue failure and elastic stresses are variable for the turbine blades with different crystal orientations. So, it is paramount to achieve the crystal orientations of arbitrary turbine blades before processing numerical calculations for them. Until now, two methods, which are Electro-Back Scattered Diffraction (EBSD) and Rotating Orientation X-Ray Diffraction (RO-XRD), have been developed to measure the crystal orientation of turbine blades with anisotropy materials.[7-9] Both methods can provide approximate results in measuring the crystal orientation angles. However, increasing the withdrawal velocity will result in a higher misorientation during directional solidification and a higher initial deviation will cause a more severe increase in misorientation after withdrawal transition. Besides, complex and expensive equipment is essential in the measuring process for previously developed methods.

In this paper, a method based on enhanced mode basis is developed to linearly express the mode shapes of arbitrary turbine blades. The proposed enhanced mode basis can be effectively used for modal analysis of blades with arbitrary crystal orientations. Surrogate model based on Kriging method is also introduced for solving the eigenproblem of blades under arbitrarily distributed crystal orientation with high efficiency and accuracy during the process. Finally, genetic algorithm is employed to identify the crystal orientations of turbine blades by optimizing the defined fitness functions that were constructed by considering the variation of frequencies and correlation of mode shapes.

The content of this paper is arranged as follows: in the first section, characteristics of turbine blades with anisotropy materials and some previous work on the crystal orientation identification are briefly presented; in the second section, the properties of blades with anisotropy materials are described and the construction of enhanced mode basis are explored. Furthermore, the identification process based on surrogate model and the genetic algorithm are provided; Then, various examples of numerical studies are utilized to demonstrate the validity of the proposed method; conclusions are drawn and discussion is made in the end.

2. Method for crystal orientation identification

2.1. Blades with anisotropy materials

The single crystal and directionally solidified superalloys can be modelled as orthotropic material properties. The orthotropic material is expressed with three mutually perpendicular axes of symmetry and nine independent material coefficients.[10-11] The compliance matrix, $\boldsymbol{E}^{\mathrm{C}}$, is usually defined by the so-called engineering constants: E_i is Young's moduli for tension-compression with respect to the directions of orthotropic axes; v_{ij} is the Poisson's ratio for the transverse strain in the *j*th direction when the material is stressed in the *i*th direction; G_{12}, G_{13} and G_{23} are the shear moduli for the planes of coordinate axes designed by subscripts, as Eq.(1). For SC alloys, the elements, $\left(E_i, G_{ij}, v_{ij}\right)$, of the compliance matrix are the same in three perpendicular directions *X*, *Y* and *Z*. For directionally solidified alloys, however, these kinds of materials are transversely isotropic. For example, DS alloys have one isotropic plane and the same values of engineering constants corresponding to transverse, namely, $E_2 = E_3$, $G_{12} = G_{13}$, $v_{12} = v_{13}$ and the directions of subscript 1 and 2 with transverse plane are according.

$$\boldsymbol{E}^{\mathrm{C}} = \begin{bmatrix} \frac{1}{E_1} & -\frac{v_{12}}{E_1} & -\frac{v_{13}}{E_1} & 0 & 0 & 0 \\ & \frac{1}{E_2} & -\frac{v_{23}}{E_2} & 0 & 0 & 0 \\ & & \frac{1}{E_3} & 0 & 0 & 0 \\ & & & \frac{1}{G_{12}} & 0 & 0 \\ & & & & \frac{1}{G_{13}} & 0 \\ \text{Sym.} & & & & & \frac{1}{G_{23}} \end{bmatrix} \tag{1}$$

According to the generalised Hook's law, the stiffness matrix, $\boldsymbol{D}$, and compliance matrix, $\boldsymbol{E}^{\mathrm{C}}$, are related as

$$\boldsymbol{D}=\left(\boldsymbol{E}^{\mathrm{C}}\right)^{-1} \tag{2}$$

Practically, the primary axis of blades is usually within a cone spanning up to 15° of the stacking line as shown in Fig.1. And the coordinate transformation of stress and strain between two Coordinate Systems (CS) is as follows:

$$\{\boldsymbol{\sigma}\}_{\mathrm{G}}=\boldsymbol{T}_{\sigma}\{\boldsymbol{\sigma}\}_{\mathrm{M}};\{\boldsymbol{\varepsilon}\}_{\mathrm{G}}=\boldsymbol{T}_{\varepsilon}\{\boldsymbol{\varepsilon}\}_{\mathrm{M}} \tag{3}$$

where the subscript G and M denote the specimen and material coordinate systems, respectively; $\boldsymbol{T}_{\sigma}$ and $\boldsymbol{T}_{\varepsilon}$ are formulated as[6]

$$\boldsymbol{T}_{\sigma}=\begin{bmatrix} l_1^2 & m_1^2 & n_1^2 & 2l_1m_1 & 2m_1n_1 & 2n_1l_1 \\ l_2^2 & m_2^2 & n_2^2 & 2l_2m_2 & 2m_2n_2 & 2n_2l_2 \\ l_3^2 & m_3^2 & n_3^2 & 2l_3m_3 & 2m_3n_3 & 2n_3l_3 \\ l_1l_2 & m_1m_2 & n_1n_2 & l_1m_2+l_2m_1 & m_1n_2+m_2n_1 & n_1l_2+n_2l_1 \\ l_2l_3 & m_2m_3 & n_2n_3 & l_2m_3+l_3m_2 & m_2n_3+m_3n_2 & n_2l_3+n_3l_2 \\ l_3l_1 & m_3m_1 & n_3n_1 & l_3m_1+l_1m_3 & m_3n_1+m_1n_3 & n_3l_1+n_1l_3 \end{bmatrix} \tag{4}$$

$$\boldsymbol{T}_{\varepsilon}=\begin{bmatrix} l_1^2 & m_1^2 & n_1^2 & l_1m_1 & m_1n_1 & n_1l_1 \\ l_2^2 & m_2^2 & n_2^2 & l_2m_2 & m_2n_2 & n_2l_2 \\ l_3^2 & m_3^2 & n_3^2 & l_3m_3 & m_3n_3 & n_3l_3 \\ 2l_1l_2 & 2m_1m_2 & 2n_1n_2 & l_1m_2+l_2m_1 & m_1n_2+m_2n_1 & n_1l_2+n_2l_1 \\ 2l_2l_3 & 2m_2m_3 & 2n_2n_3 & l_2m_3+l_3m_2 & m_2n_3+m_3n_2 & n_2l_3+n_3l_2 \\ 2l_3l_1 & 2m_3m_1 & 2n_3n_1 & l_3m_1+l_1m_3 & m_3n_1+m_1n_3 & n_3l_1+n_1l_3 \end{bmatrix} \tag{5}$$

where l_i, m_i and n_i are direction cosines between material-CS and specimen-CS of turbine blades. Moreover, the position of the material system (x, y, z) with respect to the specimen system (X, Y, Z) is determined by the direction cosines shown in Table 1. Therefore, when the alignment of two coordinate systems is not exactly parallel, the varied stiffness matrix, $\boldsymbol{D}_{\mathrm{G}}$, is

$$\boldsymbol{D}_{\mathrm{G}}=\boldsymbol{T}_{\sigma}\boldsymbol{D}\boldsymbol{T}_{\varepsilon}^{-1} \tag{6}$$

Table 1 Direction cosines

Direction	X	Y	Z
x	l_1	m_1	n_1
y	l_2	m_2	n_2
z	l_3	m_3	n_3

For the description of two coordinate systems, we adopt the first kind of Eulerian angles, where the order of three involving rotations are: (A) the first rotation is by the angle ψ about the Z axis of specimen system; (B) the second rotation is by the angle θ about X' axis of the first rotated system; (C) the third rotation is by the angle φ about Z axis of the second rotated system, as shown in Fig.2. In Cartesian coordinate system, the transformation matrices with respect to Z and X axes are as follows[12-13]:

$$\begin{cases} \boldsymbol{R}_Z=\begin{bmatrix} \cos\alpha & \sin\alpha & 0 \\ -\sin\alpha & \cos\alpha & 0 \\ 0 & 0 & 1 \end{bmatrix} \\ \boldsymbol{R}_X=\begin{bmatrix} 1 & 0 & 0 \\ 0 & \cos\alpha & \sin\alpha \\ 0 & -\sin\alpha & \cos\alpha \end{bmatrix} \end{cases} \tag{7}$$

where α is the generalised rotation angle with respect to the corresponding specified axis. With the stipulated Eulerian angles, the final rotation matrix $\boldsymbol{R}$, can be achieved by multiplying the three order rotation transformation matrices as

$$\boldsymbol{R}=\boldsymbol{R}_Z(\varphi)\boldsymbol{R}_X(\theta)\boldsymbol{R}_Z(\psi) \tag{8}$$

In consequence, the direction cosines between two coordinate systems can be obtained as[14]

$$\begin{cases} l_1 = \cos\psi\cos\varphi - \sin\varphi\sin\psi\cos\theta \\ l_2 = -\cos\psi\sin\varphi - \sin\psi\cos\varphi\cos\theta \\ l_3 = \sin\psi\sin\theta \\ m_1 = \sin\psi\cos\varphi - \cos\psi\sin\varphi\cos\theta \\ m_2 = -\sin\varphi\sin\psi - \cos\psi\cos\varphi\cos\theta \\ m_3 = -\cos\psi\sin\theta \\ n_1 = \sin\varphi\sin\theta \\ n_2 = \cos\varphi\sin\theta \\ n_3 = \cos\theta \end{cases} \tag{9}$$

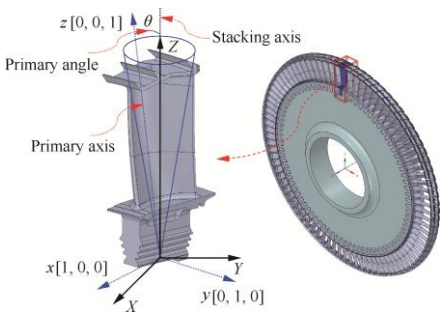

Fig. 1 Material (x, y, z) and specimen (X, Y, Z) coordinate systems.

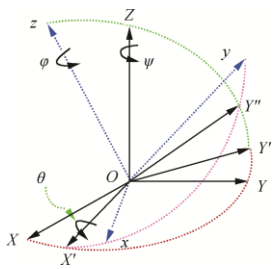

Fig. 2 Eulerian angles involving three rotations.

2.2 Modal properties of blades with arbitrary crystal orientations

The eigenproblem for turbine blades has the form:

$$\left(\boldsymbol{K}+\delta\boldsymbol{K}\right)\tilde{\boldsymbol{\Phi}}=\left(\boldsymbol{M}+\delta\boldsymbol{M}\right)\tilde{\boldsymbol{\Phi}}\tilde{\boldsymbol{\Lambda}} \tag{10}$$

where $\boldsymbol{K}$ and $\boldsymbol{M}$ are the stiffness and mass matrices of original turbine blades, i.e. the material-CS of turbine blades exactly parallels to specimen-CS; $\delta\boldsymbol{K}$ and $\delta\boldsymbol{M}$ are the perturbed matrices of stiffness and mass due to variation of material-CS with respect to specimen-CS; $\tilde{\boldsymbol{\Lambda}}$ and $\tilde{\boldsymbol{\Phi}}$ are the eigenvalue and eigenvector matrices, correspondingly. Actually, the crystal orientation variation only has influence on the stiffness of blades, while the mass is constant. So, the perturbed matrix of stiffness is a function of varied angles while the perturbed matrix of mass is a full zero matrix, i.e. $\delta\boldsymbol{K}=\delta\boldsymbol{K}\left(\psi,\theta,\varphi\right)$, $\delta\boldsymbol{M}=\boldsymbol{0}$.

Practically, the turbine blades inevitably suffer from angle variation of crystal orientation, which leads to different stiffness perturbed matrices for arbitrary blade. The enhanced mode basis has been deliberately established to

represent the modal properties of arbitrary turbine blades. Namely, the mode shapes of turbine blades with arbitrary crystal orientation can be approximately expressed as a linear combination of enhanced mode basis:

$$\tilde{\boldsymbol{\Phi}} = \left[\boldsymbol{\Phi}_1, \boldsymbol{\Phi}_2, \cdots, \boldsymbol{\Phi}_n\right]\boldsymbol{c} = \boldsymbol{\Phi}_{\mathrm{E}}\boldsymbol{c} \tag{11}$$

where $\boldsymbol{c}$ is the coefficient matrix of blade mode shapes expanded over the enhanced mode basis; $\boldsymbol{\Phi}_j \left(j = 1, 2, \cdots, n\right)$ is a set of mode shapes obtained by blades with different crystal orientations; $\boldsymbol{\Phi}_{\mathrm{E}}$ is the notation of the enhanced mode basis. Substituting Eq. (11) into Eq. (10) and pre-multiplying the transposition of enhanced mode basis, the eigenproblem equation can be formulated as

$$\boldsymbol{\Phi}_{\mathrm{E}}^{\mathrm{T}}\left(\boldsymbol{K} + \delta\boldsymbol{K}\right)\boldsymbol{\Phi}_{\mathrm{E}}\boldsymbol{c} = \boldsymbol{\Phi}_{\mathrm{E}}^{\mathrm{T}}\boldsymbol{M}\boldsymbol{\Phi}_{\mathrm{E}}\boldsymbol{c}\tilde{\boldsymbol{\Lambda}} \tag{12}$$

where only the stiffness perturbed matrix $\delta\boldsymbol{K}$, is unknown for arbitrary provided crystal orientations of turbine blades, when the eigenproblem is solved.

By the presented rotation way shown in Fig.2, CS & DS alloys are both transversely isotropic. It is explicit that the primary angle is equal to the second order rotation angle, θ, and the first and third order rotation angles, ψ and φ, describe the position of a cone with a conical angle, θ, and the rotation level, φ, around its primary axis. For the turbine blade with single crystal and directionally solidified alloys, the position of primary axis is critical and it primarily influences its mechanical behavior such as the natural frequencies, mode shapes, stress and strain, etc. Generally, to meet the properties of anisotropic blades and visualize the primary axis in a planar polar figure for convenience, the primary angle, θ, and its circumferential position, β, referenced to X axis are presented. The circumferential position angle, β, under the introduced rotation order can be derived from Eq. (9) as

$$\beta = -\arctan\left(\cot\psi\right) \tag{13}$$

when we calculate the angle, β, the limit of angle from anti-tangent solution should be taken into account. The visualized figure of the primary axis description and notations is shown in Fig.3(a). In the picture, three red circles are presented and show primary axes of three blades. The primary angles, θ, and circumferential angles, β, in plane of these three blades are (5°, 10°, and 15°) and (0°, 120°, and 240°), respectively.Based on the visualization of primary angle position, the construction of enhanced mode basis, $\boldsymbol{\Phi}_{\mathrm{E}}$, is shown in Fig.3(b). Generally, the enhanced mode basis is constructed by a large number of mode sets of blades. Considering the requirements of accuracy and efficiency in calculation, the number of mode sets is usually truncated with optimal efficiency. Here the enhanced mode basis is constructed by a mode set obtained from the blade without any variation of primary axis and four mode sets obtained from the blade whose primary angle is 13° and uniformly distributed in the circumferential position, that is, the number of enhanced mode sets is 5, i.e. $n = 5$ in Eq. (11).

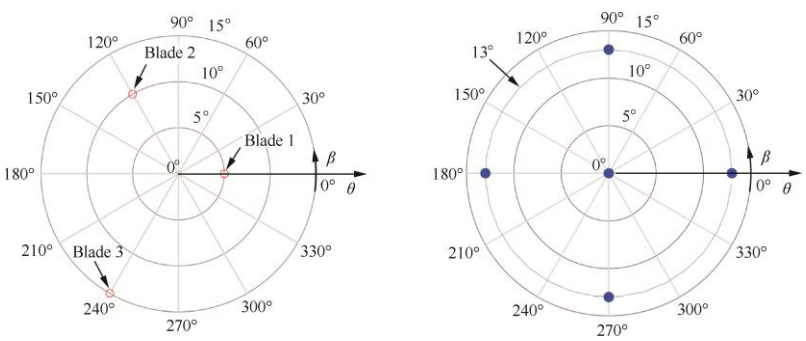

(a) The primary axis description and notations (b) Construction for enhanced mode basis

Fig. 3 Plan visualization of primary axis position

2.3 Crystal orientation identification based on surrogate model and genetic algorithm

For convenience, Eq. (12) can be rewritten as

$$\left(\mathcal{K}_{\mathrm{o}}+\delta\mathcal{K}\right)\boldsymbol{c}=\mathcal{M}\boldsymbol{c}\tilde{\boldsymbol{\Lambda}} \quad (14)$$

where $\mathcal{K}_{\mathrm{o}}=\boldsymbol{\Phi}_{\mathrm{E}}^{\mathrm{T}}\boldsymbol{K}\boldsymbol{\Phi}_{\mathrm{E}}$, $\delta\mathcal{K}=\boldsymbol{\Phi}_{\mathrm{E}}^{\mathrm{T}}\delta\boldsymbol{K}\boldsymbol{\Phi}_{\mathrm{E}}$ and $\mathcal{M}=\boldsymbol{\Phi}_{\mathrm{E}}^{\mathrm{T}}\boldsymbol{M}\boldsymbol{\Phi}_{\mathrm{E}}$ denote the corresponding condensed matrix of original stiffness matrix, perturbed stiffness matrix and mass matrix of turbine blades respectively. The enhanced mode basis can be obtained from blades with crystal orientations shown in Fig.3(b). In addition, the enhanced mode basis is constant and can be used for arbitrary blades with any crystal orientation. So, $\mathcal{K}_{\mathrm{o}}$ and $\mathcal{M}$ are constant matrices for any case. In order to efficiently describe the condensed matrix of stiffness perturbation, the Kriging method[15-16] is introduced to approximate the condensed perturbed matrix $\delta\mathcal{K}$. The dimension of $\delta\mathcal{K}$ depends on the modal truncation number, i.e. the total dimension is 5 times the modal truncation number for the construction of the enhanced mode basis as shown in Fig.3(b). So, it is efficient to perform the approximation of elements of matrix $\delta\mathcal{K}$. Under the ordering of the defined Eulerian angles, only the first two angles (ψ,θ) are important for the dynamic characteristics of turbine blades, so the condensed perturbed matrix is formulated as

$$\delta\mathcal{K}=\delta\mathcal{K}\left(\psi,\theta\right) \quad (15)$$

and moreover $\delta\mathcal{K}=\left[\delta\mathcal{K}\right]^{\mathrm{T}}$, so only the elements of upper/lower triangle of the condensed perturbed matrix need to be approximated.

When the surrogate model is constructed based on Kriging method for the condensed perturbed stiffness matrix $\delta\mathcal{K}$, the employed design points are visualized in Fig.4. Because the elements of $\delta\mathcal{K}$ are complex functions of angles θ and β, the total number of design points is 361 (i.e. the angles θ and β within the considered range are uniformly partitioned into 11 and 36 points), which can obtain enough accuracy for approximating the elements of the condensed stiffness perturbed matrix with higher efficiency. Consequently, for an arbitrary blade, the eigenproblem of Eq. (14) can be solved directly based on $\delta\mathcal{K}$ that is achieved from a surrogate model with the corresponding crystal orientation of this turbine blade.

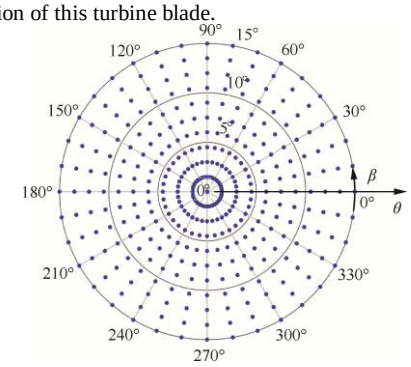

Fig. 4 Crystal orientation distribution of design points for surrogate model construction.

For exactly identifying the crystal orientation with high efficiency, genetic algorithm is employed[17-18]. The modal information of blades is used to construct the fitness functions of genetic algorithm. The variations of modal properties obtained from Eq. (14) based on the surrogate model with respect to the unidentified structure are quantified as

$$\begin{cases}\kappa\left(\psi,\theta\right)=\sum_{i=1}^{m}\left(\mathrm{Freq}_i-\mathrm{freq}_i\right)/\mathrm{freq}_i\\ \xi\left(\psi,\theta\right)=\sum_{i=1}^{m}\left(1-\mathrm{MAC}_{ii}\right)\end{cases} \quad (16)$$

where Freq_i is the frequency of the ith mode obtained from Eq. (14), i.e. searching from constructed surrogate model; freq_i is the frequency of the ith mode of an unidentified blade; m is the number of modal truncation; MAC_{ii} is the Modal Assurance Criterion (MAC) of the ith mode between mode shapes obtained from Eq. (11) and from the unidentified blade. The MAC values can be obtained as[19]

$$\mathrm{MAC}_{ij}=\frac{\left|\{\boldsymbol{\phi}_{\mathrm{A}}\}_i^{\mathrm{T}}\{\boldsymbol{\phi}_{\mathrm{B}}\}_j\right|^2}{\left(\{\boldsymbol{\phi}_{\mathrm{A}}\}_i^{\mathrm{T}}\{\boldsymbol{\phi}_{\mathrm{A}}\}_i\right)\left(\{\boldsymbol{\phi}_{\mathrm{B}}\}_j^{\mathrm{T}}\{\boldsymbol{\phi}_{\mathrm{B}}\}_j\right)} \tag{17}$$

where i and j denote the index of modes; $\boldsymbol{\phi}_{\mathrm{A}}$ and $\boldsymbol{\phi}_{\mathrm{B}}$ denote the mode shapes of two compared structures respectively.

Consequently, considering the variations of modal properties between that achieved from Eq. (14) and from the unidentified blade, construction of three kinds of fitness functions for genetic algorithm is introduced and formulated as follows:

$$\begin{cases} f_1=\kappa(\psi,\theta)\times 100 \\ f_2=\xi(\psi,\theta)\times 100 \\ f_3=\left[\kappa(\psi,\theta)+\xi(\psi,\theta)\right]\times 100 \end{cases} \tag{18}$$

The procedure of crystal orientation identification based on surrogate model and genetic algorithm is described as follows:

(1)Construct the surrogate model based on Kriging method for condensed perturbed matrix of stiffness, $\delta\mathcal{K}$. And, calculate the condensed matrices $\mathcal{K}_{\mathrm{o}}$ and $\mathcal{M}$ using enhanced mode basis with nominal/initial stiffness and mass matrices.

(2) Prepare the modal properties (frequencies and mode shapes) for unidentified structures.

(3) Optimize the fitness functions in Eq. (18) using genetic algorithm tool. The crystal orientation angles are identified when steady convergence emerges.

3. Numerical studies

3.1 Accuracy of enhanced mode representation and surrogate model

In this section, the accuracy of using an enhanced mode basis to represent the mode shapes of turbine blade with arbitrary crystal orientation and the description of the condensed perturbed matrix, $\delta\mathcal{K}$, by using a surrogate model are demonstrated. In general, the first 30 modes are considered for calculation in this paper. The anisotropy material employed for numerical calculations is DZ125[20-21] and the employed blade model is shown in Fig. 5. This turbine blade model has about 47000 Degrees of Freedoms (DoFs) and is meshed by Solid 187 in ANSYS. The boundary condition of the blade is set to be fixed at the root.

The accuracy of frequencies by using enhanced mode basis to express modes of arbitrary turbine blades is shown in Fig. 6 (a). From this picture, the maximum error of the first 30 modes is less than 0.0026%. The MAC values between the mode shapes derived from Eq. (11) and that from directly solving the finite element model of blade are plotted in Fig. 6 (b). The diagonal elements of MAC matrix are all equal to 1. It illustrates high accuracy of the proposed method by using an enhanced mode basis to linearly represent the mode shapes of arbitrary turbine blades with anisotropy materials.

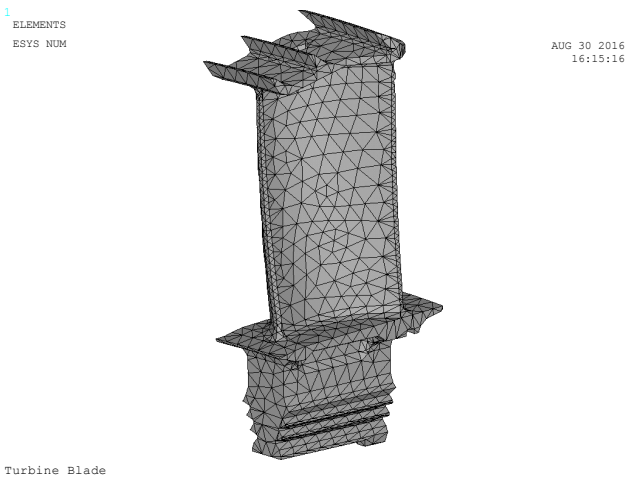

Fig. 5 Finite element model of employed turbine blade.

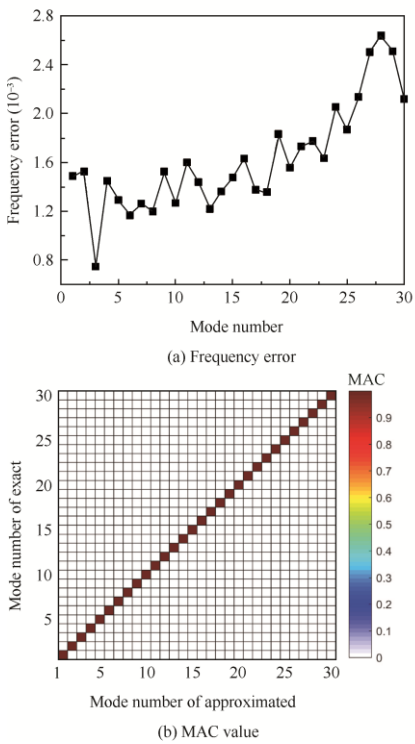

Fig. 6 Accuracy of enhanced mode representation versus original finite element model

In order to perform the modal analysis of Eq. (14) in high efficiency, Kriging method is introduced to construct a surrogate model for the elements of the condensed perturbed matrix $\delta\mathcal{K}$. For visualizing the variation of elements of the condensed perturbed matrix with respect to the position of primary axis, θ and β, the variation distribution of the first element of matrix $\delta\mathcal{K}$ is shown in Fig.7. The variation values are normalized to the maximum component. The variation distribution of other elements of condensed perturbed matrix possesses the same complex varied properties. Actually, any element of $\delta\mathcal{K}$ has a surrogate model as shown in Fig.7, but the

variation distribution is different when the upper/lower triangle of matrix is considered (because $\delta\mathcal{K}$ is a symmetric matrix).

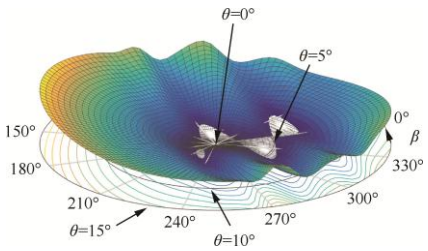

Fig. 7 Normalized variation distribution of the 1st element of condensed perturbed stiffness matrix.

In order to illustrate the accuracy of the surrogate model based on Kriging method, an example is employed. The surrogate model is constructed as the previously mentioned method. Frequencies obtained from the directly-condensed perturbed matrix with respect to those from the condensed perturbed matrix based on the surrogate model are compared and the corresponding errors are shown in Fig. 8(a). It can be seen that the maximum error from the surrogate model is less than $6.0\times10^{-6}\%$, almost no error being introduced by employing the surrogate model. Furthermore, the MAC values corresponding to this case are shown in Fig. 8(b). It is shown that all the diagonal components of MAC matrix are equal to 1. That is, both mode shapes obtained from the directly-condensed perturbed matrix and from the condensed perturbed matrix based on the surrogate model are in good agreement. Therefore, the surrogate model based on Kriging method for the condensed perturbed matrix is demonstrated with high accuracy and efficiency and shows significant advantage for approximating the elements of the condensed perturbed matrix.

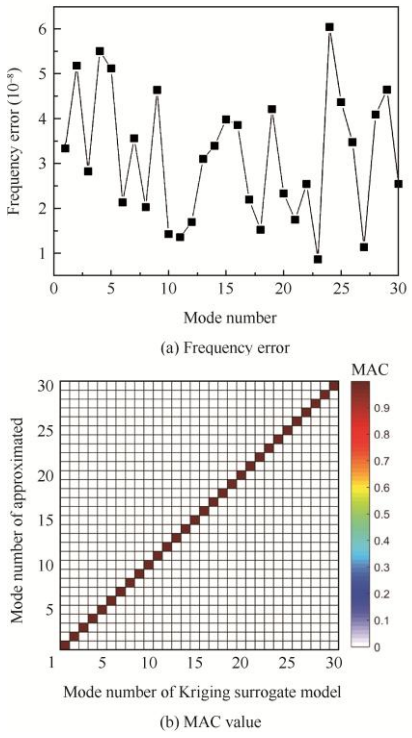

Fig. 8 Accuracy of surrogate model versus original model

3.2 Examples of crystal orientation identification

The process of crystal orientation identification is based on the surrogate model and genetic algorithm. Thereinto, surrogate model is employed to achieve the condensed perturbed matrix of stiffness for Eq. (14) of blades with arbitrary crystal orientation, while the genetic algorithm is used to search the optimal value of fitness functions. Comprehensively, constructions of three fitness functions are employed to separately identify the crystal orientation angles as Eq.(18). For options of genetic algorithm, the number of population is 50; the number of iteration is 15 (because 15 iterations can achieve convergence for three kinds of fitness functions). Various optimizations below are discussed to investigate the identification capability of the proposed method by using different fitness functions:

(A) The fitness function only considers the variation of frequency as f_1: From Eq.(18), four cases with different combinations of angles ψ and θ are discussed. The convergence curves of these four cases are plotted in Fig. 9(a). Obviously, the fitness functions in four cases all converge to a steady value after 10 iterations.

(B) The fitness function only considers the percentage variation of MAC values as f_2. The relationships between the fitness function value and the iteration number in four cases above are overlaid in Fig. 9(b). It can be seen clearly that in all cases convergence is achieved after several or over ten iterative processes.

(C) The fitness functions, f_1 and f_2, are both considered as f_3: When considering both variation of frequencies and modal assurance criterion of mode shapes in the fitness function, the iterative process still converges in four cases as shown in Fig. 9(c). Clearly, when the number of iterations is equal to 15, four cases are all converged to a steady value.

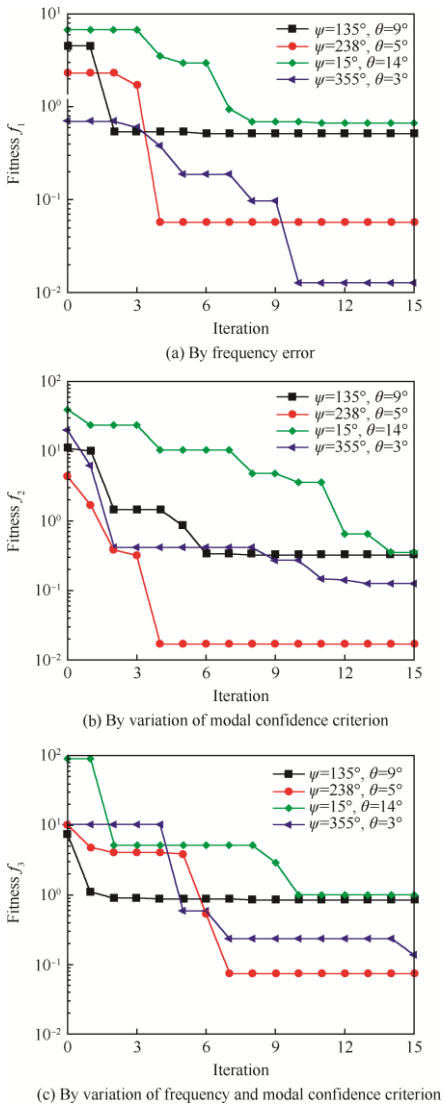

Fig. 9 Convergences of fitness functions constructed by three different ways.

From Fig. 9, it can be seen that the convergence rates among three different fitness functions are different. The fitness function only considering the frequency information converges in the fastest rate, while the one considering both frequency and mode shapes simultaneously converges slowly. In summary, identification results of these four cases are provided in Table 2. The fitness functions constructed as f_1, f_2 and f_3 can exactly identify the crystal orientation angles, ψ and θ, although time consumption of these three fitness functions is quite different. The fitness function constructed based on the frequency variation is considered preponderant within 82 s for 15 iterations.

Table 2 Parameters of crystal orientation identification.

Case (°)		Converged iteration			Time for 15 iteration (s)			Identified conclusion		
ψ	θ	f_1	f_2	f_3	f_1	f_2	f_3	f_1	f_2	f_3
135	9	3	6	9	82	290	409	Yes	Yes	Yes
238	5	4	4	7				Yes	Yes	Yes
15	14	8	14	10				Yes	Yes	Yes
355	3	10	13	15				Yes	Yes	Yes

4. Conclusions and discussion

The method of enhanced mode basis has been developed to linearly express the mode shapes of arbitrary turbine blades with any crystal orientation variation of anisotropy materials. The proposed method can be utilized for blades with any stiffness perturbed matrix, with high accuracy and efficiency.

Surrogate model based on Kriging method has been introduced for solving the eigenproblem of blades with crystal orientation arbitrarily distributed. The solution is highly effective and efficient without any loss of accuracy.

Genetic algorithm has been employed to optimize the defined fitness functions, which were constructed by considering the variation of frequencies and correlation of mode shapes. The crystal orientation angles are identified according to the convergence curves of fitness functions.

A computer program for identification of crystal orientation for turbine blades with anisotropy materials has been developed. The accuracy and the computational efficiency of the proposed method have been demonstrated with a realistic turbine blade on several random cases.

There are still several issues that require further exploration. For example, an effective procedure of finite element modelling including the mesh quality and the trusted fixed conditions is required, and the experimental test to capture the effective modal information of turbine blades with anisotropy materials in order to validate the proposed method is also essential. Nowadays, the non-contact measurement, such as the scanning laser Doppler vibrometry, that is capable of measuring the natural frequencies and the detailed mode shapes of a structure in a fast way, looks very promising. The techniques of modeling error identification, model correlation and updating similarly show great potential to validate the practical application of the proposed method. The further research on these issues is currently underway and the results will be reported in another paper in the future.

Acknowledgements

This work was co-supported by the National Natural Science Foundation of China (Nos. 51405460, 11372128 and 51175244) and National Safety Academic Foundation of China (No.U1730129). The supports from the Collaborative Innovation Center of Advanced Aero-Engine, Jiangsu Province Key Laboratory of Aerospace Power System, the Key Laboratory of Aero-Engine Thermal Environment and Structure, Ministry of Industry and Information Technology are also gratefully acknowledged.

References

1. Manetti M, Giovannetti I, Pieroni N, Horculescu H, Peano G, Zonfrillo, G, et al. The dynamic influence of crystal orientation on a second generation single crystal material for turbine buckets. *ASME turbo expo 2009: Power for land, sea, and air* ;2009.p.125-33.
2. Chang JC, Yun YH, Choi C. Failure analysis of gas turbine buckets. *Engineering Failure Analysis* 2003;10(5):559-67.
3. Kiyak Y, Fedelich B, May T. Simulation of crack growth under low cycle fatigue at high temperature in a single crystal superalloy. *Engineering Fracture Mechanics* 2008;75(8): 2418-43.
4. Savage MWR. The influence of crystal orientation on the elastic stresses of a single crystal nickel-based turbine blade. *ASME 2011 turbo expo: Turbine technical conference and exposition*; 2011.p.37-46.
5. Kaneko Y. Study on vibration characteristics of single crystal blade and directionally solidified blade. *ASME 2011 turbo expo: Turbine technical conference and exposition* ; 2011.p.931-40.

6. Arakere NK, Swanson GR. Effect of crystal orientation on fatigue of single crystal nickel base turbine blade superalloys. *Journal of Engineering for Gas Turbines & Power* 2000, 124(1):V004T01A004.
7. Sadeghi F, Kermanpur A, Sarami N, Heydari D, Nematollahi J, Bahmani M. A comparison on the EBSD and RO-XRD techniques for measuring crystal orientation of the single-crystal Ni-based superalloys. *Metallography Microstructure & Analysis* 2016:5(4) :1-8.
8. Ai C, Zhou J, Zhang H. Misorientation induced by withdrawal rate transition and its effect on intermediate temperature stress rupture properties of a Ni3Al based single crystal superalloy. *Journal of Alloys and Compounds* 2015; 637:77-83.
9. Guo Z, Fu T, Fu H. Crystal orientation measured by XRD and annotation of the butterfly diagram. *Materials Characterization*, 2000;44(4):431-4.
10. Petrov E, Géradin M. Finite element theory for curved and twisted beams based on exact solutions for three-dimensional solids part 2: anisotropic and advanced beam models. *Computer Methods in Applied Mechanics & Engineering* 1998 ； 165(1–4)：93-127.
11. Skrzypek JJ, Ganczarski AW. *Mechanics of anisotropic materials*. Berlin: Springer International Publishing; 2015.p.87-129.
12. Slabaugh GG. Computing Euler angles from a rotation matrix. *Retrieved on August* 1999,6(2000)：39-63.
13. Piovan G, Bullo F. On coordinate-free rotation decomposition: Euler angles about arbitrary axes. *IEEE Transactions on Robotics* 2012;28(3): 728-33.
14. Lesk† AM. On the calculation of Euler angles from a rotation matrix. *International Journal of Mathematical Education in Science and Technology* 1986;17(3):335-7.
15. Lophaven SN, Nielsen HB, Søndergaard J. DACE—A MATLAB Kriging toolbox—version 2.0," Kgs. Lyngby, Denmark :Technical University of Denmark; 2002. Report No. IMM-REP-2002-12.
16. Couckuyt I, Forrester A I, Gorissen D. Blind Kriging: Implementation and performance analysis. *Advances in Engineering Software*, 2012;49(1) :1-13.
17. Boussaid I, Lepagnot J, Siarry P. A survey on optimization metaheuristics. *Information Sciences* 2013: 237:82-117.
18. Konak A, Coit D W, Smith A E. Multi-objective optimization using genetic algorithms: A tutorial. *Reliability Engineering & System Safety* 2006, 91(9): 992-1007.
19. Pastor M, Binda M, Harcarik T. Modal assurance criterion. *Procedia Engineering* 2012; 48(1):543-8.
20. Hu XA, Yang XG, Shi DQ, Yu HC, Ren TT. Constitutive modelling of a directionally solidified nickel-based superalloy DZ125 subjected to thermal mechanical creep fatigue loadings. *Rare Metals* 2016.p. 1-15.
21. Hu XA, Yang XG, Shi DQ, Yu HC. Out of phase thermal mechanical fatigue investigation of a directionally solidified superalloy DZ125. *Chinese Journal of Aeronautics* 2016, 29(1): 257-67.